CDF/MEMO/PUBLIC/5873
March 23, 2002

A Preliminary Study of Beam Halo and Beam Radiation Sources in CDF

R.J. Tesarek
Fermilab, Batavia, IL 60510

Abstract

Using a simple set of scintillator telescopes, we make preliminary measurements of beam halo and beam related radiation sources inside the CDF collision hall. These data indicate that the low beta quadrupoles form a line source of beam related radiation. The halo surrounding the beamline is dominated by particles following the proton direction and is 7–45 times larger than the halo associated with anti-protons. The overall halo rates are significantly larger on the west side of the detector than on the east.

1 Introduction

Since the startup of the run II program, CDF has encountered significant problems with VME power supply failures and muon chamber currents which have been attributed to radiation in the CDF collision hall. To better understand the nature of the radiation environment in the collision hall, a series of scintillator telescopes were set up in the collision hall. A description of the measurements made and preliminary conclusions follows below.

2 Measurement Technique

We used telescopes composed of pairs of scintillation counters to view potential sources of beam related radiation. The scintillator counters used for these measurements come from a pool of spares originally manufactured in 1994 for the muon identification and veto hodoscopes in the KTeV experiment. The active volume (scintillator) for these counters measures $1.3 \times 15.0 \times 150.0$ cm^3. A solid lucite light guide is attached to one end of the scintillator and mates to an EMI-9954KB photomultiplier

Figure 1: Diagram of the KTeV scintillator counters used for these measurements.

Table 1: Scintillator counter operating parameters.

Counter Name	Counter ID	PMT bias Voltage (V)	Attenuation Length(m)	Dark Count Rate(Hz)
A	102	1816	245 ± 21	53
B	003	1788	255 ± 23	284
C	042	1896	237 ± 20	30
D	059	1637	241 ± 21	185

tube (PMT). The opposite end of the scintillator was painted black to avoid light reflections. Figure 1 is a diagram of the counters used for these measurements. Descriptions of the counter performance characteristics may be found in references [1, 2, 3].

On arrival in CDF, the counters were inspected and light leaks repaired. Bias voltages for the counter PMTs were set 100 V above the knee of plateau curves made at the time of production using a 30 mV discriminator threshold. At the above setting, measurements in the KTeV hall of similar counters operated in the same fashion found an inefficiency of 1×10^{-5}. The dark (singles) rates were measured with the above discriminator thresholds. Table 1 summarizes the operating parameters of the counters used in these measurements.

The counters were arranged into telescopes in one of 3 different configurations. The first configuration (see Figure 2) pointed three telescopes at two of the low beta quadrupoles on the east side of the CDF detector and at the pole face between the quadrupole. This configuration is used to establish the rate of backscattered protons from the quadrupole pole face relative to large angle backward scatters from the quadrupoles. The last two configurations (see Figures 3) retained one of the original telescopes for normalization and formed two additional telescopes looking for halo parallel to the beam in the proton and antiproton directions on either side of the CDF detector.

The logic for the telescopes was set up such that signals from pairs of counters

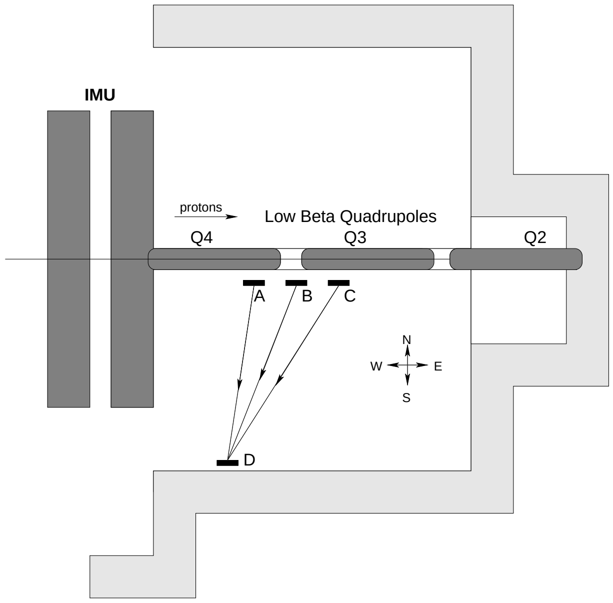

Figure 2: Telescope configuration 1. Only the east side of the CDF collision hall is represented.

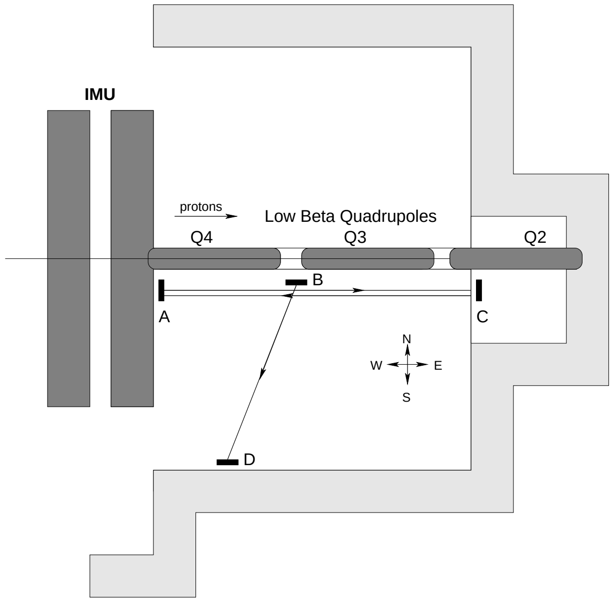

Figure 3: Telescope configuration 2. The telescopes formed by counters A-C were moved to the west side of the detector for configuration 3.

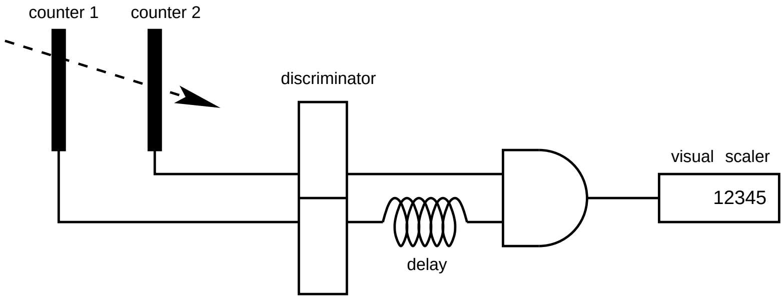

Figure 4: Schematic diagram of the logic used for a single telescope.

Table 2: Summary of relative delays and acceptances of telescopes in the configurations listed.

Config.	Telescope	dist. (m)	Delay(ns)	Accept
1	A $\rightarrow$ D	4.85	16	1.22
	B $\rightarrow$ D	5.21	17	1.00
	C $\rightarrow$ D	6.02	20	0.72
2	A $\rightarrow$ C	7.59	25	1.00
	C $\rightarrow$ A	7.59	25	1.00
3	A $\rightarrow$ C	7.59	25	1.00
	C $\rightarrow$ A	7.59	25	1.00

forming a telescope were discriminated (threshold=30 mV, width=10 ns) and set in a delayed coincidence. The coincidence was formed so that the discriminated signal from the counter closest to the proposed source was delayed relative to the signal from the second counter. The amount of the delay was calculated as the distance between the pair of counters divided by the speed of light. The coincidence signals were then sent to visual scalers. Figure 4 is a schematic of the logic used for one telescope.

Rates were then measured by sending a 10 second gate simultaneously to the four scalers and dividing the resulting counts by 10. Several measurements were taken every few hours during a store. In order to compare the rates for the counters on an equal footing, the relative acceptances had to be calculated for the telescopes in the first configuration. The telescope formed by the counters B–D was used for normalization of both the acceptances and eventually the rates. Table 2 summarizes the distance between counters,the relative delay between counters in the telescopes and the relative acceptance between the different telescopes. All coincidence rates were measured without beam and found to be well below 0.05 Hz, independent of the configuration.

The telescopes were set up in configuration 1 for store 919. Telescopes A–D and C–D measured the rate of backward scattered particles from the bodies of the two low beta quadrupoles, Q4 and Q3, while telescope B–D measured the rate of backward scatters from the pole faces of Q3. Figure 5 compares the acceptance corrected telescope rates with the luminosity and beam losses for various times during the store. For stores 1002 and 1036, the telescopes were set up in configurations 2,3. In these configurations, the telescopes A–C and C–A measured particles parallel to the proton and antiproton directions while telescope B–D remained unchanged. Figures 6,7 compare the telescope rates with luminosity and beam losses during the stores. Because the B–D telescope was common for all studies, one may compare results from the different configurations. Table 3 summarizes the telescope rates in the early portions of each store normalized to the B–D telescope viewing the Q3 pole faces.

Table 3: Summary of rates in all telescopes from the early portion of each store normalized to the B-D telescope viewing the pole faces of the Q3 low beta quadrupole. The uncertainties quoted are statistical.

Config	Store	telescope	Comment	Rate(Hz)	Relative rate
1	919	A-D	Q4	2534	0.711 ± 0.010
		B-D	Q3 pole face	3563	1.000 ± 0.000
		C-D	Q3	2359	0.662 ± 0.014
2	1002	A-C	proton(east)	103783	8.939 ± 0.008
		C-A	pbar(east)	2522	0.217 ± 0.010
		B-D	Q3 pole face	11610	1.000 ± 0.000
3	1036	A-C	proton(west)	103223	9.257 ± 0.060
		C-A	pbar(west)	14441	1.295 ± 0.010
		B-D	Q3 pole face	11151	1.000 ± 0.000

3 Discussion

One may draw some preliminary conclusions from these data. The time dependence of the telescope rates appears to more closely follow the CDF luminosity than the losses. At this time, it is unknown why the time dependence between losses and telescope rates appear to be different.

For the telescopes in configuration 1, the backward scatters originating from the low beta quadrupoles Q3, Q4 are only 30% less than the backward scatters from the Q3 pole face. The east/west low beta quadrupole strings are each enclosed in a common cryostat. The difference in rates of the three telescopes is most likely to be due to the amount of material the scattered particles traverse than a dominance of backscattered particles from the quadrupole magnet pole faces. These data would indicate that the quadrupoles form a line source in the CDF collision hall.

The data from the telescopes in configurations 2,3 indicate that halo surrounding the proton beam dominates. The relative halo rates between the protons and antiprotons appear to depend on whether one monitors the east or west side of the detector.

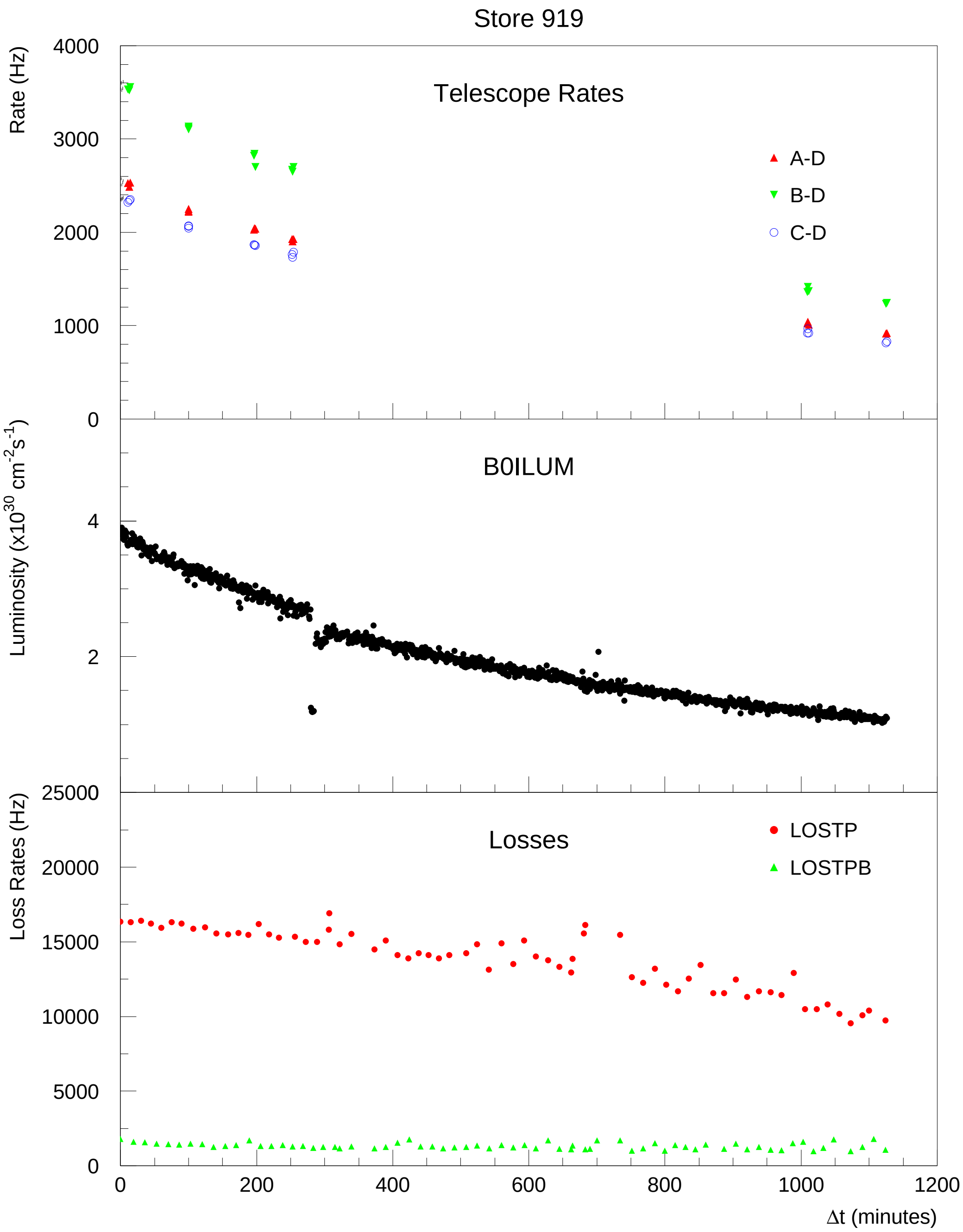

Figure 5: Corrected telescope rates from configuration 1(top), luminosity (middle) and beam losses (bottom) as a function of time for store 919. Telescopes A–D, B–D and C–D point at Q4, Q3 pole face and Q3 respectively. The early portion of the store has been omitted.

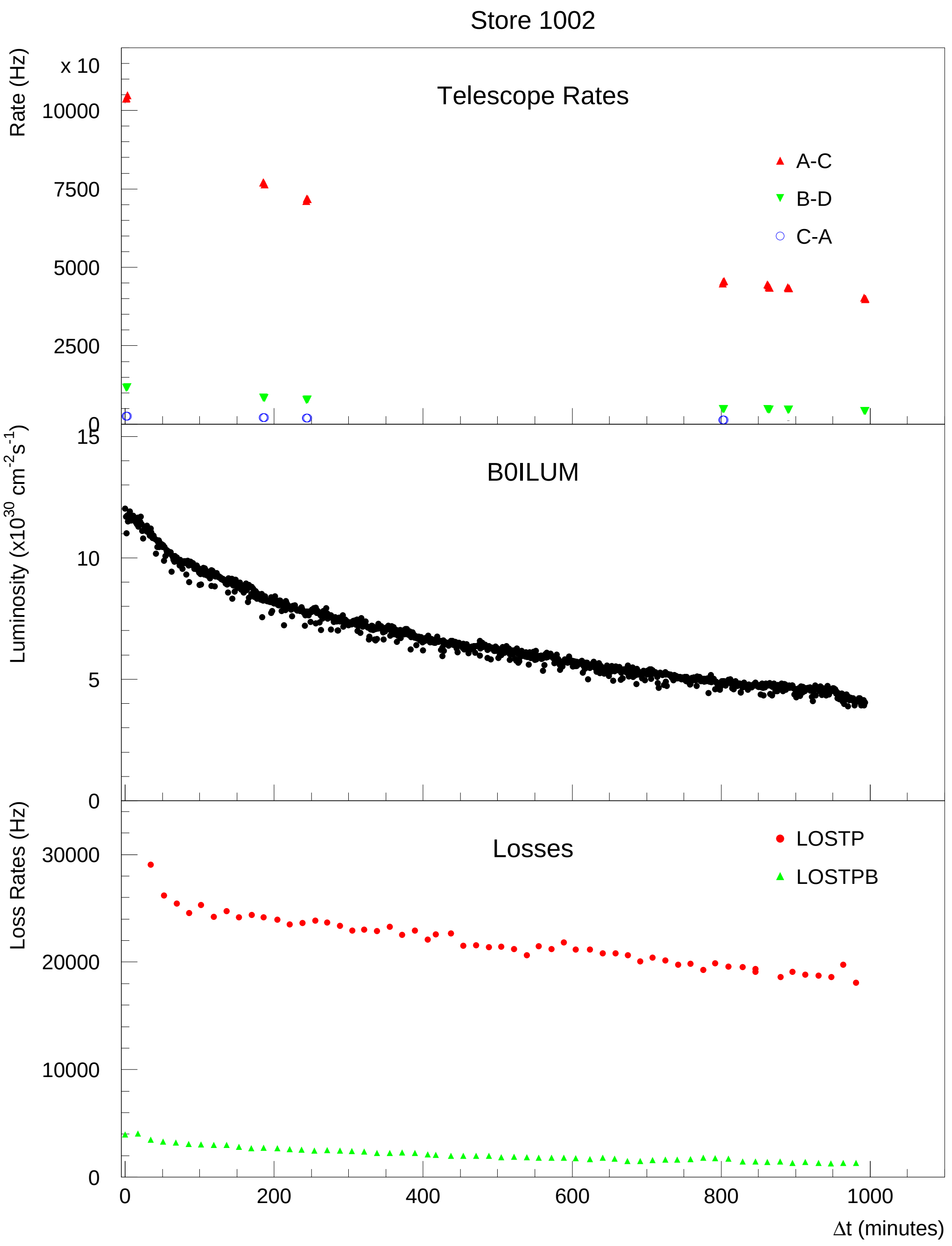

Figure 6: Corrected telescope rates from configuration 1(top), luminosity (middle) and beam losses (bottom) as a function of time for store 1002. Telescopes A–C and C–A point in the proton and antiproton directions while telescope B–D points at the Q3 pole face. The early portion of the store has been omitted.

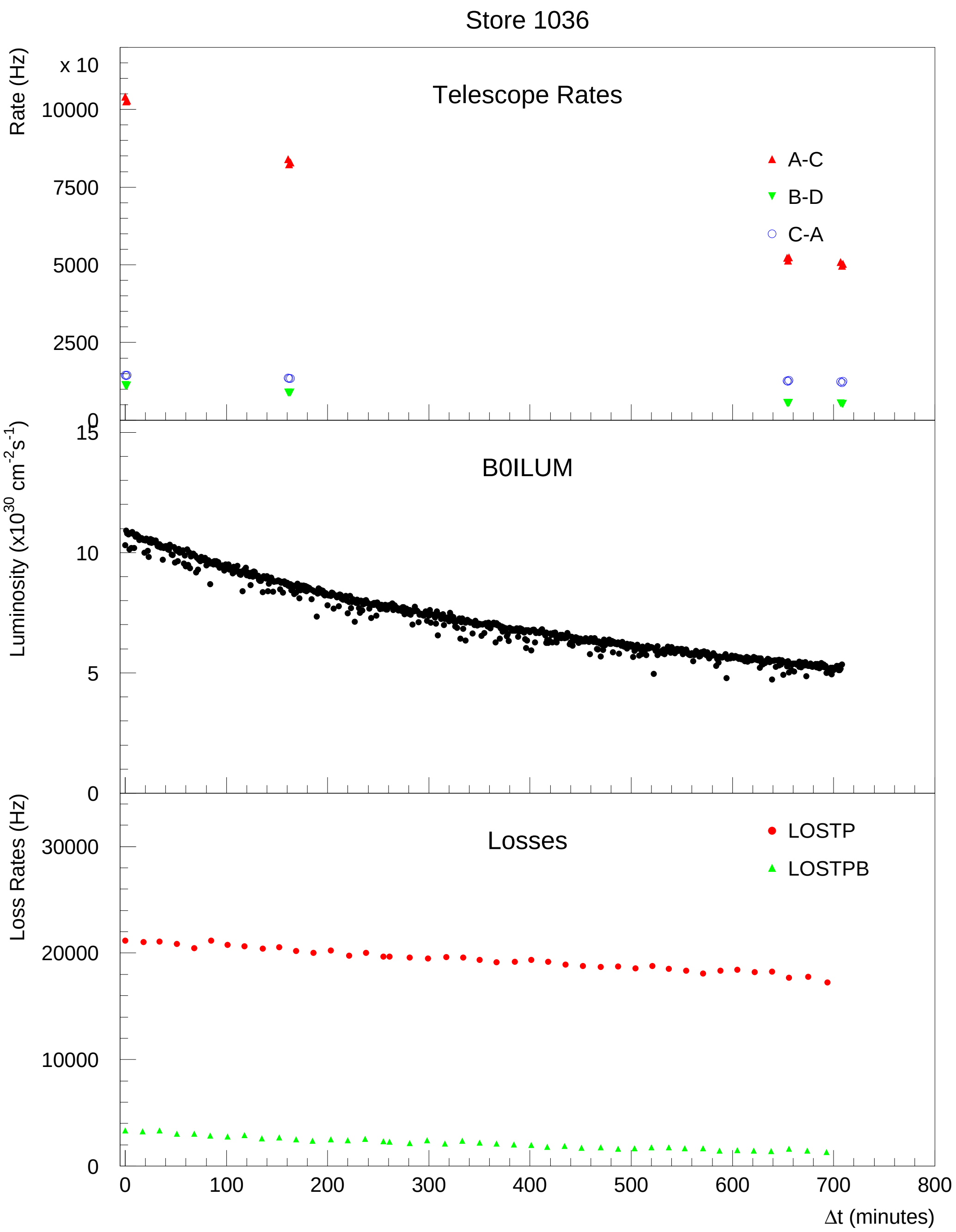

Figure 7: Corrected telescope rates from configuration 1(top), luminosity (middle) and beam losses (bottom) as a function of time for store 1036. Telescopes A–C and C–A point in the proton and antiproton directions while telescope B–D points at the Q3 pole face. The early portion of the store has been omitted.

The proton/pbar halo ratio was seen to vary over the range 7–45.

4 Conclusions

Early measurements of beam related radiation sources were made using simple scintillator telescopes arranged in three different configurations. Data from these telescopes indicate that the CDF low beta quadrupoles form a line source of radiation. As expected, protons tend to produce the dominant contributions to this radiation. These measurements were unable to observe the contribution of collisions to the proton halo to the east of the detector. Collisions tend to dominate the antiproton halo to the west of the detector.

References

[1] R.J. Tesarek, “Muon Counter Gain Calibration and Tracking in E832,” KTeV internal note, KTEV-0389, 11 February 1997.

[2] R.J. Tesarek, “Muon Counter Time Calibration and Stability in 1996 E832 Data” KTeV internal note, KTEV-0429, 10 June 1997.

[3] R.J. Tesarek, “Muon System Hardware Trigger Efficiency,” KTeV internal note, KTEV-0481, 25 November 1997.